Research Article | Vol. 27, No. 5 | 4 Mar 2019 | OPTICS EXPRESS 7602
Optics EXPRESS

Infinite deflectometry enabling 2π-steradian measurement range

L. R. GRAVES,[1] H. QUACH,[1] H. CHOI,[1] AND D. W. KIM[1,2,*]

[1]College of Optical Sciences, University of Arizona, 1630 E. University Blvd., Tucson, AZ 85721, USA
[2]Steward Observatory, University of Arizona, 933 N. Cherry Ave., Tucson, AZ 85719, USA
* letter2dwk@hotmail.com

Abstract: We present a novel deflectometry implementation termed Infinite Deflectometry. The technique provides a full aperture surface reconstruction sag map of freeform surfaces, including previously challenging to measure optics such as highly convex surfaces. The method relies on the creation of a virtual source enclosure around the tested optic, which creates a virtual 2π-steradian measurement range. To demonstrate the performance, a fast f/1.26 convex optical surface was measured with a commercial interferometer and with the Infinite Deflectometry system. After removing Zernike terms 1 through 37, the metrology tests resulted in absolute RMS surface values of 18.48 nm and 16.26 nm, respectively. Additionally, a freeform Alvarez lens was measured with the new technique and measured 22.34 μm of surface sag RMS after piston, tip/tilt, and defocus had been removed. The result deviated by 488 nm RMS from a profilometer measurement while standard interferometry failed to measure the Alvarez lens due to its non-nulled wavefront dynamic range limitation.

1. Introduction

While freeform optics provide ever-growing possibilities in designing cutting edge optical systems, their fabrication and metrology remain challenging. Currently, a wealth of fabrication methods exists whose variety provide improved fabrication of freeform surfaces. Such methods include computer numeric controlled (CNC) machining using a diamond tip tool, sub-aperture polishing using a magnetorheological fluid (MRF), molded optics, precision polishing, and more [1–5]. In verifying the freeform shape generated, two commonly utilized non-contact optical metrology methods for a unit under test (UUT) are interferometry and deflectometry [6,7].

Interferometry, which offers high accuracy and precision in surface metrology, requires a null setup to obtain accurate test results of a UUT. Computer generated holograms (CGHs) are increasingly chosen as null components in interferometric tests for their abilities to precisely create a freeform null wavefront, and, in some cases, provide additional alignment features [8,9]. Unfortunately, CGHs can be prohibitively expensive and can only null a designed specific configuration. Alternatively, deflectometry is a non-null test method which has been shown to provide surface metrology accuracy similar to commercial interferometry systems for freeform optics [7,10–12]. The method relies on rays leaving a source, being deflected by a UUT, and then being recorded by a camera. In this way, the local slopes across the UUT are measured, which can be used to reconstruct the surface through integration.

One subset of optics that still is highly challenging to measure is convex optics, both standard in shape as well as freeform. There exist a variety of test methods, including interferometric approaches, swing arm profilometry, and the Hindle test [13–15]. Most methods typically require measuring sub-apertures of the unit, which are then 'stitched' together. Great improvements have been made in interferometry algorithms which lead to improved sub-aperture stitching results [14,16–18]. Unfortunately, having an interferometric setup and the required null optic is not always a viable option. Further, spatial sampling of the surface shape can be limited with other metrology techniques such as contact-type

#358219 https://doi.org/10.1364/OE.27.007602
Journal © 2019 Received 21 Jan 2019; revised 17 Feb 2019; accepted 17 Feb 2019; published 28 Feb 2019

Optics EXPRESS

profilometers, negatively impacting the mid-to-high spatial frequency measurement capability.

While traditional deflectometry has been used as a 3D object reconstruction method for surfaces up to and including weak (i.e., large radius of curvature) convex surfaces, a full aperture optical precision test of a general convex surface has not been achieved. However, there have been successful methods which measure a plano-convex optic in transmission [19], as well as using a unique scanning laser deflectometry system to measure the departure from a sphere of convex aspheric surfaces [20]. The fundamental limitation to testing a surface using traditional deflectometry is satisfying a line of sight condition. When considered in reverse, if a ray from the camera can be traced to a point on the optical surface and, following the law of reflection, passes through the source area, the optical surface slope can be determined at said location. Traditionally, for a concave test using deflectometry, the source and camera will be placed as close to the center of curvature as possible [21,22]. This allows a small area on the source (e.g., small liquid crystal display [LCD] screen) to fully satisfy the line of sight condition. However, as the optical surface transitions from concave towards convex, the source area must increase to satisfy the line of sight condition. One work-around is instead to surround the optical surface with the screen. One implementation of this concept, known as 'Cavlectometry', has successfully been used to reconstruct low order surface shapes of objects such as the hood of an automobile and a teapot [23]. In this approach, a projector system was used to project phase-shifted fringes onto the walls of a room in which the tested object sat. The system is thus able to achieve an extremely large source area which encloses the UUT.

An array of projectors is not the only possible method for creating a source enclosure. While a projector array can nicely satisfy the need to create a source enclosure around the UUT, projectors systems suffer from lower resolution, optical aberrations, contrast uniformity, and more [24,25]. This in turn adds uncertainty to the deflectometry system, which can limit reconstruction accuracy. Modern digital displays possess characteristically higher resolution but are also limited by realizable source sizes. In a new configuration, a high-resolution source enclosure may be achieved by seating a UUT atop a precision rotation stage which clocks the UUT, while a digital screen and camera are mounted in place. Here, each clocked position generates a new 'virtual' deflectometry system, which is equivalent to rotating a single tilted display and camera about the UUT. By using multiple clocking positions, a series of 'virtual' screens can be created which entirely enclose the UUT, creating a tipi-shaped 2π-steradian measurement space. This is the fundamental concept of Infinite Deflectometry (ID).

In this paper we present a novel optical quality deflectometry method which generates a full aperture surface map of a unit under test. The method uses the 'Cavlectometry' model as inspiration, but instead creates a source enclosure around the UUT by means of a series of 'virtual' high resolution digital displays. This allows for high accuracy testing of fully freeform surfaces, including previously unachieved optical quality full-aperture surface metrology maps of convex surfaces using deflectometry. This method, termed 'Infinite Deflectometry', to reflect an 'infinite' dynamic range (practically limited by camera line of site), was used to measure both a highly convex spherical optic and an Alvarez lens. Results demonstrate a close match between full-aperture interferometric testing results for the convex spherical optic. Additionally, the Alvarez test results suggest this new branch of deflectometry expands the range of testable surfaces without necessitating a custom null component.

2. Background theory

2.1 Phase shifting deflectometry

Phase shifting deflectometry is a popular metrology method for testing optics [7,21,22,26–29]. The technique calculates the local slopes on a UUT using a camera and a digital display.

Optics EXPRESS

The camera is positioned to image the UUT surface. The camera pixels have their 3D location recorded, defined as x_c, y_c, z_c, and the pixels are mapped to the UUT surface. The mapped pixels represent discrete areas on the UUT where the local slopes will be calculated, known as 'mirror pixels'. The 3D location of the UUT and specifically the precise location of the mirror pixels is determined for the test, defined as x_U, y_U, z_U. The digital source displays a sinusoid pattern in the x and y directions, using a minimum of 3 phase steps. The reflected light is captured by the camera and the recorded wrapped phase is acquired. The phase is unwrapped and the precise location on the source which successfully illuminated every camera pixel corresponding to its mirror pixel is determined. By relating these to the location of the display, the 3D location of the display points corresponding to the camera detector pixels is determined, known as x_S, y_S, z_S. Using these three data matrices, the local slopes in the x and y orthogonal directions of the UUT at the discrete 'mirror pixels' are calculated. Finally, the local slopes are integrated, typically using a zonal integration method such as a Southwell integration [30]. In this way, the surface is reconstructed from a deflectometry slope measurement.

2.2 Infinite deflectometry creating virtual source

The deflectometry test method as described is a non-null metrology method. Two key aspects limit the range of surface slopes that the system can practically measure. First, the camera must have a clear line of sight to the area on the UUT that is to be measured. Second, if the camera pixels are traced from the camera to the UUT surface and deflected, following the law of reflection, the rays must pass through the defined source (i.e., screen) area. While the traditional deflectometry method works well for most concave surfaces, as the required source area is small by performing the test near the center of curvature, it struggles to test optical surfaces as they move away from a concave shape. As the UUT surface has a wider range of slopes, typical for freeform surfaces, or as the surface moves towards a flat or convex shape, the required source area to cover the UUT rapidly becomes very large. One work around proposed is to enclose the UUT with the source [23], thus allowing for testing a wider range of surface slopes. Figure 1 demonstrates the challenges associated with testing a convex surface with a traditional deflectometry setup and how a source enclosure could expand the testable surface range.

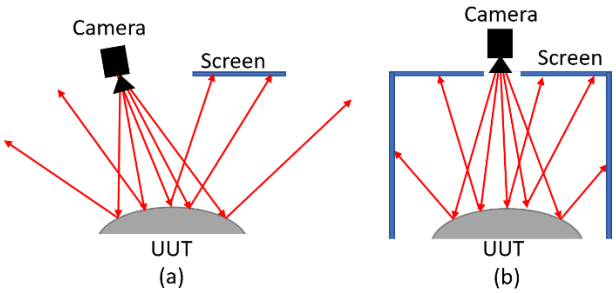

Fig. 1. A traditional deflectometry system utilizes a camera and source to test a UUT. If considered in reverse, rays can be traced from the camera to the UUT where they are deflected by the UUT mirror surface and, if they pass through the source area, the local slope on the UUT can be determined using geometry. For some surfaces, such as a convex optic, a regular screen is not large enough to allow for testing the full area of the UUT due to the missing rays (a) and presents an area where deflectometry has historically not been able to provide full aperture metrology maps. One alternative is a source screen which encloses the UUT, allowing for testing the full range of surface slopes without missing rays (b).

A modern LCD is a common source used in a deflectometry setup, desirable for their high resolution and stability. Depending on the system architecture and the optic under test there is a limit to the testable dynamic range of surface slopes for the UUT for given display size and

Optics EXPRESS

resolution. The testable dynamic range increases as the size of the display increases, but there is a limit to the size of display that can reasonably be obtained. While a monolithic box-shaped screen which encloses the UUT would be ideal, no such screen exists in practice. Utilizing a projector system is one alternative, but there are significant distortion, uniformity, and mapping challenges associated with projectors, which limit their usability for high precision nanometer scale optical tests.

Instead of increasing the size of the screen, a series of virtual screens has been generated in the Infinite Deflectometry system. In this way, the benefit of a small high-resolution display can be leveraged while at the same time creating a larger source area. To achieve this, a source display is positioned tilted over the UUT, with a camera positioned over the UUT to image the surface. To generate a virtual screen, the UUT is clocked by a fixed angular step, which presents new areas of the UUT to the screen and camera. After a full 2π rotation of clocking steps, this can equivalently be thought of as generating a tipi-shaped virtual screen. This process is repeated to create overlapping virtual screens which entirely enclose the optic, thus allowing for the entire range of surface slopes to be tested. It should be noted that the ability to create the virtual screen enclosure is limited by the size of the UUT and the available source. For extremely large UUTs, even the largest commercially available screen will not be able to fully virtually enclose the UUT in the described configuration. Figure 2 demonstrates the setup concept, and how one high-performance screen which can test only a limited area on the UUT can be turned into six virtual screens to enclose the UUT.

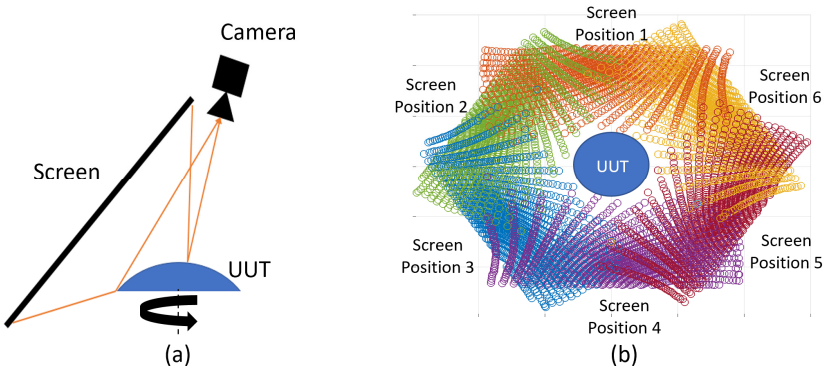

Fig. 2. By tilting a high precision screen over a UUT, and correctly positioning the camera, a partial area of the UUT can be measured using traditional deflectometry (a). If the UUT is placed on a precision rotation stage and clocked to multiple angular orientations (e.g., 6 screen positions), the full area of the UUT can be tested. This can be thought of as instead virtually clocking the screen and camera, creating a virtual source enclosure allowing for the same precision metrology over the full UUT aperture. Because each screen can only cover a segment of the UUT, a reverse ray trace from the camera pinhole to the UUT is performed to determine the intercept locations with the virtual screens, seen from the top down as scattered points (b).

At each clocking position, a deflectometry measurement is performed which covers a partial section of the UUT. After recording the data, the local slopes are calculated for every virtual configuration. This is done by carefully determining the 3D positions of the camera, screen, and UUT in the default unclocked test position, which are described as matrices which contain the individual local x, y, z positions previously discussed and are referred to as C_0, S_0, and U_M respectively. It should be noted that U_M represents an accurate model of the UUT whose center position defines the global coordinate system. During processing, for the first clocked testing position, the camera and base screen position matrices are rotated about the UUT optical axis by the amount the UUT was clocked during the test, creating new 3D position matrices. The new virtual camera position matrix is referred to as C_1 and following the phase unwrapping process the local screen positions are correlated to the global screen

Optics EXPRESS

position, and the new virtual screen position matrix, S_1, is determined. This process is repeated for every clocking position, which for *N* clocking positions of the UUT results in a total of *N* (0 to *N*-1) camera and source 3D position matrices. When this process is completed, *N* deflectometry test data sets exist, and the local slopes for every test are determined. This is accomplished by tracing the camera pixels for every camera matrix $C_{0:N-1}$ to U_M, the UUT model, to determine the local ray intercept locations. These local ray intercept points, which are the x_U, y_U, z_U coordinates for every clocking position, are stored in matrices $U_{0:N-1}$. Knowing the final ray locations, which are recorded as the x_S, y_S, z_S in screen matrices $S_{0:N-1}$, the local slopes on the UUT model for every virtual test system in the global x and y directions are determined and recorded as $X_{0:N-1}$ and $Y_{0:N-1}$ respectively.

To combine the data into cohesive x and y local slope maps of the UUT, a multi-step process is used. First, due to uncertainty in positioning of components, there exist some uncertainties associated with the positions determined for all components in the system. These errors most heavily dominate low spatial frequency shapes, particularly piston, tip and tilt, defocus, and astigmatism. Therefore, these terms are removed from the local slope maps by subtracting the mean values of the local slopes and then performing a best fit plane to the data and subtracting this away as well. In the spatial domain, the mean of the local slopes represents the tip/tilt (depending on if it is the x or y data) while the plane fit to the data represents the first derivate of the surface, corresponding to the defocus and astigmatism of the surface. It is worth mentioning that, fundamentally, this uncertainty can be reduced with more thorough calibration and higher accuracy hardware components, which broadly is true for all general stitching metrology system cases.

After this step, the data is combined by performing linear interpolation fitting which takes the x and y UUT intercept locations and the adjusted local slope data for every test and generates a single cohesive x and y slope map of the UUT. The x and y slope maps are generated over a uniform grid. The local slopes were averaged for positions where the ray intercepts overlapped for two or more sub-aperture local slope measurements. The local slope maps in the x and y directions of the entire UUT surface are referred to as T_X and T_Y respectively. It must be noted that because the subaperture local slope maps have the slopes determined in the global coordinate system, all subaperture local slope maps are in the same reference frame. A Southwell integration [30] is then performed on T_X and T_Y which results in a reconstructed surface sag map, referred to as U_R. It is important to acknowledge that the unique value and novelty of the Infinite Deflectometry is in the enhanced dynamic range enabled by the virtual tipi screen geometry, not in the general stitching performance related treatments, which has been actively studied and reported by the stitching metrology community. Figure 3 demonstrates the data processing flow from raw data acquisition to a full aperture reconstructed surface map.

Optics EXPRESS

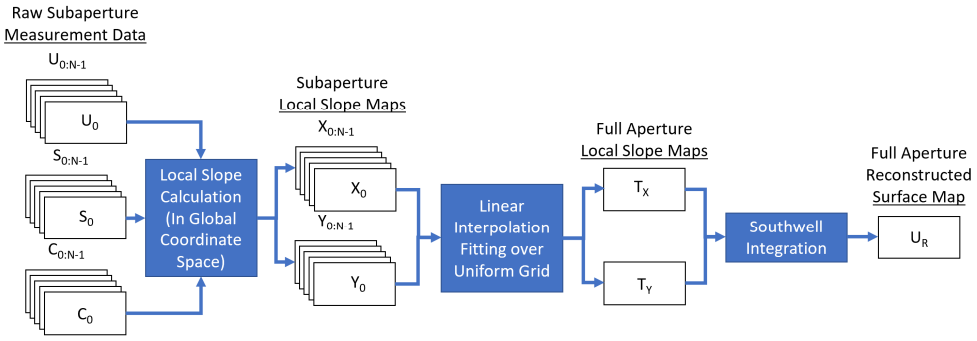

Fig. 3. Infinite Deflectometry uses a traditional deflectometry system in a unique configuration combined with clocking the UUT, which results in *N* virtual deflectometry system measurement sets, each measuring a subaperture area of the UUT. Each measurement outputs standard deflectometry outputs, resulting in global x,y,z coordinates for every test for the camera ($C_{0:N-1}$), UUT ($U_{0:N-1}$), and screen ($S_{0:N-1}$). Local slope maps in the global x and y directions for all subaperture tests are then determined, called $X_{0:N-1}$ and $Y_{0:N-1}$ respectively. A linear interpolation is used to fit the subaperture slope maps into full aperture x and y slope maps, called T_X and T_Y respectively, which are integrated using a Southwell integration to produce a full aperture reconstructed surface map of the convex UUT, called U_R.

This combined hardware and software process represents the Infinite Deflectometry technique. The method was used to test previously unmeasurable surfaces using traditional deflectometry, which demonstrate that the ID method can greatly extend the dynamic range of deflectometry to provide full aperture surface reconstruction of freeform surfaces, including flat or convex optics.

3. Experimental setup and measurements

3.1 Infinite deflectometry hardware configuration

To build and demonstrate the ID system a camera, source, and precision rotation stage were required. We utilized a Point Grey Flea3 camera (Model # FL3-U3-32S2M-CS), which has a 2.5 µm pixel pitch. This camera was utilized as its technical and mechanical data was well specified, and it had a high-resolution detector. For the source an Apple iPad Pro (Model # A1670) was utilized which measured 262.85 × 197.04 mm and had 2732 × 2048 pixels, with a 96.2 µm pixel pitch. The UUT was placed on a custom 3D printed mount, which fit into the rotation stage utilized for the test and centered the optic to the center of the rotation stage. The rotation stage was composed of a Klinger motorized rotary stage (Model # DP179), driven by a Leadshine digital stepper driver (Model # EM402).

The camera was mounted nearly centered above the UUT, while the screen was mounted in front of the UUT, and was tilted, such that the top edge of the screen slightly passed over the center of the UUT. The actual setup is shown in Fig. 3. All components were mounted on a breadboard to maintain position throughout testing. The edges of the camera body and the screen body were measured using a Coordinate Measuring Machine (CMM), accurate to ± 10 µm. Using technical drawings, the pixel positions were located relative to the camera body, while a plane was fit to the screen. The UUT body and center was measured as well, and the center of the UUT served as the global origin (0, 0, 0) coordinate. The z axis was defined as normal to the UUT and pointing up, away from the breadboard. The y axis was defined as pointing toward the screen from the UUT center, and the x axis was orthogonal to the z and y axis.

To determine the camera pointing vectors, a process previously performed was used [31,32]. The process relies on mounting the camera system such that it is pointed at a high precision monitor. The 3D position of the monitor and the camera are measured using a CMM. A line scan is performed on the monitor while the camera records. For every pixel on

Optics EXPRESS

the camera, the centroid of the measurement response is determined to precisely calculate which location on the screen was being measured by every camera pixel. The monitor was then translated along the optical axis of the camera and the process was repeated. In doing so, the precise ray vector for every camera pixel between the two screen positions could be calculated, which served as calibration of the camera ray pointing vectors. This process was performed for the camera used prior to it being mounted in the final ID system.

Once the overall assembly and the camera calibration had been performed, the ID system was used for metrology. For every clocking position, a 16-step phase shifting deflectometry (PSD) test was performed. This involved using 8 phase steps in the horizontal and vertical directions (defined by the screen) each. The entire system was shielded during all tests from stray background light by placing a heavy black cloth over the system. After a measurement was performed, the data for the clocking position was saved and then the rotation stage would rotate the UUT to the next clocking position automatically. This process was repeated until a total of *N* rotations were performed. After all data was collected the local slopes at every clocking position were determined, and full aperture local slope maps in the X and Y directions were calculated using the method described previously. These local slope maps were integrated using Southwell integration and the final reconstructed surface map was acquired.

3.2 Fast convex mirror measurement case

To verify the performance of the system, a fast f/1.26 50 mm diameter convex sphere (UUT in Fig. 4) was measured using the ID setup described. Tests using 6, 45, 90, and 180 clocking positions were performed for comparison, which are referred to as ID_R in the results section, where *R* is the number of clocking positions used, and defines the number of virtual screens which enclosed the UUT. The clocking positions were equally spaced over a full 360° to ensure maximum exposure of the UUT surface to the virtual displays. This was used to determine the as-built reconstruction performance as a function of clocking steps used.

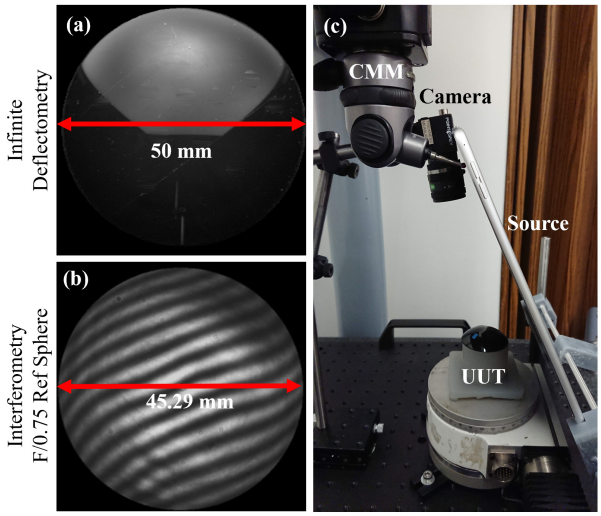

Fig. 4. A fast f/1.26 convex spherical optic with a 50 mm diameter clear aperture was measured using the Infinite Deflectometry system (a). As a comparison, a Zygo Verifire™ MST interferometer was used to provide an independent measurement of the same optic (b), which measured a maximum 45.29 mm diameter aperture inside of the 50 mm clear aperture. The Infinite Deflectometry system was composed of a camera, source, and the UUT on a rotation stage, and all components were mounted in place and measured using a CMM (c).

The test using a total of 180 clocking positions, whose reconstructed surface map is referred to as $ID_{180,}$ served as the pseudo-ideal case representing the sufficient number of

Optics EXPRESS

clocking steps. As an independent reference, the optic was measured using a Zygo Verifire™ MST interferometer which provided a comparison sag map. Due to the available reference sphere and the as-manufactured shape of the UUT, the best null configuration tested only a 45.29 mm in diameter aperture inside of the 50 mm full diameter of the optic. This measured area is referred to as INT. In all final comparisons the surface root-mean-square (RMS) data is calculated only in the common 45.29 mm inner circle of the reconstructed sag maps. The raw data images from both setups are shown in Figs. 4(a) and 4(b).

3.3 Alvarez lens measurement case

An Alvarez lens was designed and manufactured from a PMMA 1-inch diameter disk, with the optical surface machined using a diamond turning machine to generate a 6 mm central aperture area inside of the PMMA disk. The ideal optical surface was generated to have 17 µm of Zernike term Z8, which represents horizontal coma, and −17 µm of Zernike term Z10, which represents 45° trefoil. This optic represents one half of an Alvarez lens pair. Due to the non-trivial freeform nature and wide dynamic range in the surface slopes, the full aperture had previously proven very difficult to measure. For example, without a custom nulling component, such as a CGH, the fringe density exceeded the measurable range of a commercial interferometer, as shown in Fig. 5. The ID system was utilized to measure the full 6 mm central aperture, and the surface was reconstructed, referred to as $ID_{Alvarez}$.

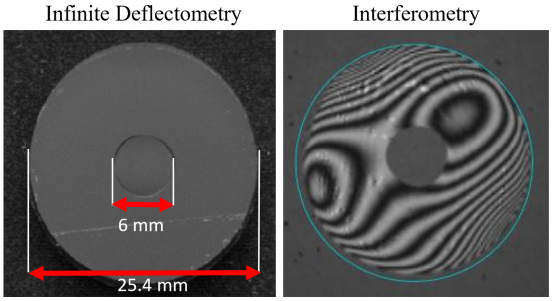

Fig. 5. An Alvarez lens was generated in a 1-inch PMMA disk. The surface was designed to have a 6 mm inner optical aperture which had 17 µm of horizontal coma and −17 µm of 45° trefoil. The surface was measured using the ID system, which measured the full aperture (left), as well using the Zygo Verifire™ MST Interferometer using a reference flat without a custom CGH (right). Without a custom null optic, the fringe density exceeded the measurement capabilities of the interferometer, making it impossible to measure the central optical aperture.

As an alternative reference comparison measurement, a contact-type KLA-Tencor Alpha-Step D-500 profilometer was utilized to measure a surface profile of the Alvarez lens. The profile line was carefully chosen to measure a profile which passed through the middle of the lens and featured primarily the coma terms. A contact force of 10 mg was utilized for the measurement in order to prevent any damage or scratch on the PMMA surface (a trial test was performed with a higher force on a separate PMMA disk and resulted in a scratch on the surface). The height range of the profilometer was limited to a maximum height deviation of 100 µm with the 10 mg force limit. It is for this reason that the profile, which measured the middle of the lens in the horizontal direction was chosen, as this profile would ideally feature heights within the measurement range while also highlighting the part of the unique surface shape of the Alvarez lens. The same profile was taken from the $ID_{Alvarez}$ reconstructed map and compared. For both profiles, the mean values of the measurements were subtracted from the raw data, thereby setting the mean for both data sets to zero for direct comparison.

Optics EXPRESS

4. Infinite deflectometry performance

4.1 Metrology results for f/1.26 50 mm diameter convex sphere

For the comparison study, piston, tip/tilt, and defocus, corresponding to standard Zernike terms 1:4, were removed from both the interferometric and ID measurements, as they are blind to those terms. Additionally, more detailed comparisons were made after standard Zernike terms 1:6 were removed, after terms 1:21 were removed, and after terms 1:37 were removed. These are referred to for the ID_R maps as $ID_R^{1:Z}$ and for the INT map as $INT^{1:Z}$, where Z refers to the highest number of standard Zernike terms removed. Finally, the surface sag root-mean-square (RMS) was calculated for the $ID_{180}^{1:Z}$, and $INT^{1:Z}$ maps over the common 45.29 mm circular aperture area of the UUT.

The reconstructed surface maps $ID_R^{1:Z}$, with Z standard Zernike terms removed and R clocking positions utilized are presented in Fig. 6. As further clocking steps are utilized in the ID system, improved reconstruction accuracy is achieved. Particularly of note are the high spatial frequencies in the reconstructed sag maps. The stitching error is most clear at high spatial frequencies when few clocking steps were used, such as in $ID_6^{1:37}$ and $ID_{45}^{1:37}$. It must be noted that for the as-built hardware used in the ID system presented here, the full test of the optic to gather the measurement data using 180 clocking is ~2 hours and 35 minutes. This does not include processing time. Thus, there is a clear tradeoff between reconstruction accuracy and time of acquisition.

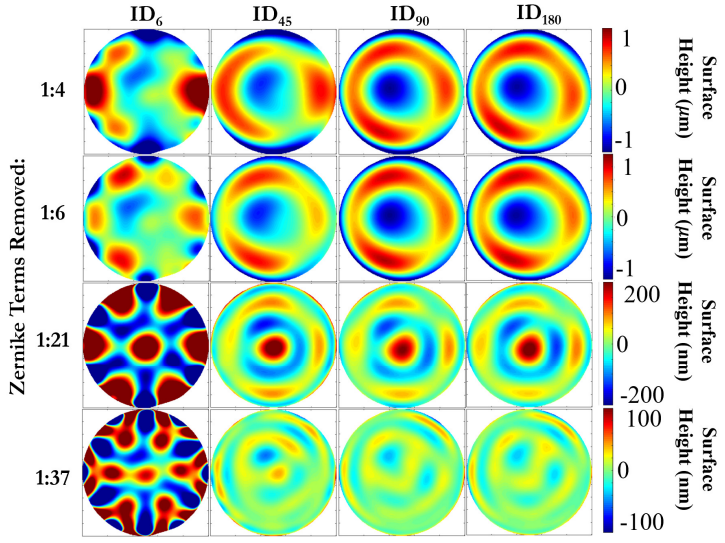

Fig. 6. The infinite deflectometry method utilizes the clocking of the UUT to create a virtual 2π-steradian tipi-shaped source area which enclose the UUT. A deflectometry test is performed at each clocking position, and the local slopes at each clocking are calculated and then stitched together to create a full aperture local slope map of the UUT, which are integrated to generate the total sag map. The process was performed for a fast f/1.26 convex sphere for 6 (1st column), 45 (2nd column), 90 (3rd column), and 180 (4th column) clocking step positions, equally spaced over a full 2π rotation. Stitching errors are apparent for fewer clocking positions, and manifest clearly as Zernike terms 1:4 (1st row), 1:6 (2nd row), 1:21 (3rd row), and 1:37 (4th row) are removed from the surface map.

The reconstructed surface maps generated by the ID metrology with 180 clocking steps, ID_{180}, and the Zygo Verifire™ MST interferometer, INT, are compared in Fig. 7 as a function of *Z* standard Zernike terms removed.

Optics EXPRESS

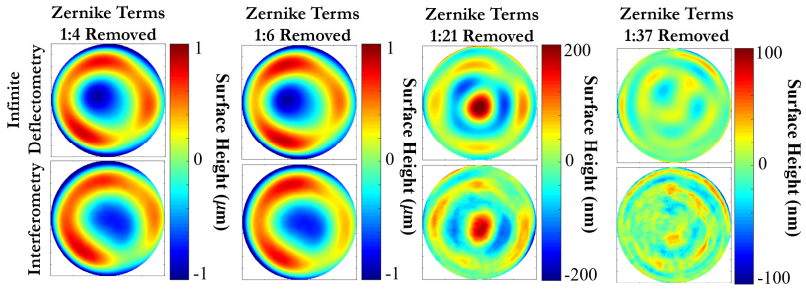

Fig. 7. A fast f/1.26 convex mirror UUT was tested using both the Infinite Deflectometry method (top row) which measured the full 50 mm diameter aperture of the UUT and a commercial Zygo Verifire™ MST interferometer (bottom row), which measured a limited measurement area of a 45.29 mm diameter aperture on the UUT. Due to uncertainties in both systems for the UUT piston, tip/tilt, and defocus, Zernike terms 1:4 were removed for both reconstruction maps (1st column). Additionally, to better compare the surface reconstruction across spatial frequencies, Zernike terms 1:6 (2nd column), 1:21 (3rd column), and 1:37 (4th column) were removed for both reconstruction maps.

The surface sag RMS values of the reconstructed maps $ID_{180}^{1:Z}$ and $INT^{1:Z}$, with Z standard Zernike terms removed, are calculated and reported in Table 1. The values were only calculated over the common 45.29 mm diameter central aperture, to match the 45.29 mm diameter aperture measured by the interferometer.

Table 1. Surface Sag RMS of 45.29 mm Diameter Central Aperture on f/1.26 50 mm Diameter Convex UUT from ID and INT Surface Sag Maps

	Surface RMS Zernike Terms 1:4 Removed (nm)	Surface RMS Zernike Terms 1:6 Removed (nm)	Surface RMS Zernike Terms 1:21 Removed (nm)	Surface RMS Zernike Terms 1:37 Removed (nm)
INT	462.04	447.69	53.71	18.48
ID_{180}	477.34	431.49	56.00	16.26

The $ID_{180}^{1:Z}$ and $INT^{1:Z}$ maps showed close agreement across spatial frequencies. Additionally, the RMS surface sage values were very similar. However, due to the overlapping areas tested and the slope stitching, it appears that the ID process performs a slight smoothing process in the reconstructed map. Additionally, some error inherent in phase-shifting deflectometry systems may be negatively impacting the reconstruction accuracy in the infinite deflectometry test. These errors, including positioning uncertainty, have been well explored for PSD based deflectometry measurements [29,33] although a more complete follow up study is required to fully understand the unique errors sources to the infinite deflecomtetry configuration. Finally, the ID process was readily able to achieve a full aperture reconstruction of the highly convex f/1.26 50 mm diameter optic, demonstrating increased testing capabilities for deflectometry.

4.2 Metrology results for Alvarez lens surface

The reconstructed map of the 6 mm optical area of the Alvarez lens as measured by the ID system, $ID_{Alvarez}$, and a comparison theoretical (i.e., designed) surface map are given in Fig. 8. Additionally, the height profile as measured by the KLA-Tencor Alpha-Step D-500 profilometer, S_P, and the height of the same profile taken from the $ID_{Alvarez}$ map, S_{ID}, are reported.

Optics EXPRESS

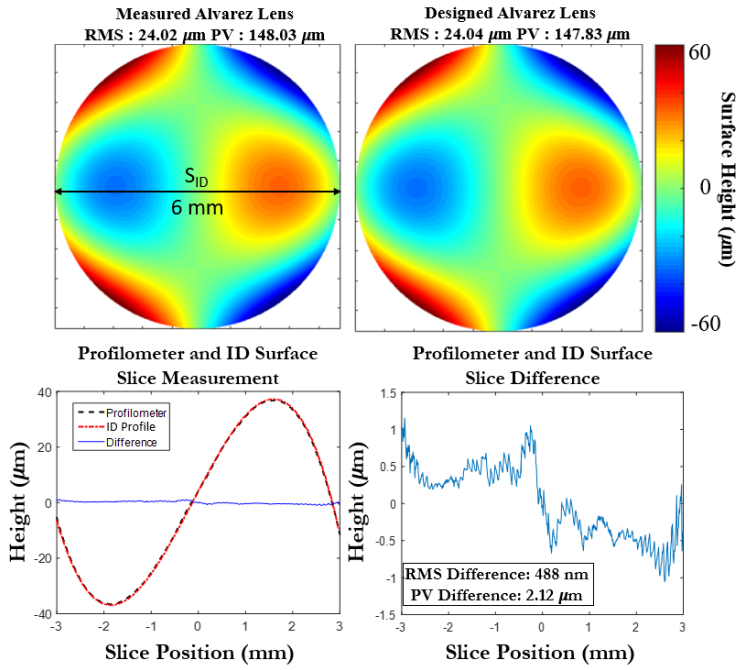

Fig. 8. An Alvarez lens represents a highly freeform surface which presents a unique metrology problem. Using a diamond turning machine a 6 mm diameter Alvarez lens with 17 µm of horizontal coma and –17 µm of trefoil was designed (top right) and manufactured. The final surface generated was measured using the Infinite Deflectometry system with 180 clocking positions (top left). To cross-check the measured data performance, a KLA Alpha-Step D-500 profilometer was used to measure a profile of the optic, shown as a black line in the surface map (top left). The surface height of the profile from the ID measurement, and the profilometer were compared (bottom left) and the difference was calculated (bottom right).

Standard Zernike terms 1:37 were fit to the $ID_{Alvarez}$ map, and the designed term values (i.e., ideal surface) are compared in Fig. 9. The RMS surface deviation from ideal design was 2.75 µm with Zernike terms 1:4 removed, 1.78 µm with terms 1:8 removed, 178 nm with terms 1:21 removed, and 160 nm with terms 1:37 removed.

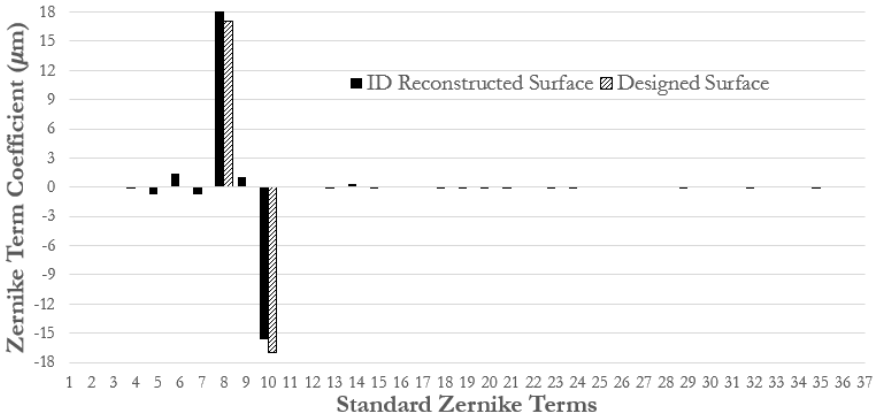

Fig. 9. Using a CNC diamond turning process, a 6 mm diameter Alvarez lens was generated on a PMMA disk and measured. The infinite deflectometry surface map was fitted with standard Zernike terms 1:37 (black bars). This was compared to the Zernike terms representing the design values (checked bars).

Optics EXPRESS

The Infinite Deflectometry system was able to achieve a full aperture surface reconstruction of the Alvarez lens, a 6 mm diameter freeform generated in a PMMA disk. The surface had ~148 μm PV of surface height variation over it. The reconstructed map was similar to the ideal surface, however, the measurement reported small amounts of Zernike terms Z5, Z6, and Z9, which represent vertical and 45-degree astigmatism and vertical trefoil respectively. Additionally, the magnitude of Z8 and Z10 in the reconstructed surface did not exactly match the designed surface. This is not unexpected for the manufacturing tolerance of machining performed for the surface. For an independent verification, a profilometer measurement of a profile of the surface was in close agreement to the same slight from the reconstructed ID surface, with 488 nm RMS difference.

5. Conclusion

While deflectometry historically has provided a powerful non-null metrology method for measuring concave optics, convex and even large flat optics have proven challenging to measure. This is due to the requirement that the source area in a deflectometry test must be large enough to allow for some light from the source to be collected by the camera, after it is deflected by the UUT. For flat to convex optics, or highly freeform optics, extremely large source areas are required to measure the full UUT area. As an alternative, we have presented Infinite Deflectometry, which utilizes a standard camera and digital display, along with a precision rotation stage which the UUT is placed upon, to create a series of virtual sources, thereby expanding the dynamic range of the slope measurement. When taken together, these virtual screens create a tipi shaped source which completely encloses the UUT and allows for testing a 'infinite' range of surface slopes.

A demonstration system successfully produced a high accuracy full aperture surface reconstruction map results of a highly convex f/1.26 50 mm diameter spherical optic, as well as testing a highly freeform Alvarez lens. The ID method represents another deflectometry system modality which extends the measurement capabilities of the deflectometry technique. We do not claim the ID method is superior to other precision metrology techniques such as interferometry. Instead, our goal is to improve the fundamental deflectometry technique to provide more value to the optics metrology community by providing multiple options and cross-checking metrology solutions.

Funding

II-VI Foundation Block-Gift Program; Technology Research Initiative Fund Optics/Imaging Program; Korea Basic Science Institute Foundation; Friends of Tucson Optics Endowed Scholarships in Optical Sciences.

References

1. M. Beier, S. Scheiding, A. Gebhardt, R. Loose, S. Risse, R. Eberhardt, and A. Tünnermann, "Fabrication of high precision metallic freeform mirrors with magnetorheological finishing (MRF)," *Optifab 2013.* International Society for Optics and Photonics **8884**, 88840S (2013).
2. S. Risse, S. Scheiding, M. Beier, A. Gebhardt, C. Damm, and T. Peschel, "Ultra-precise manufacturing of aspherical and freeform mirrors for high resolution telescopes," *Optifab 2014.* International Society for Optics and Photonics **9151**, 91510M (2014).
3. T. Blalock, K. Medicus, and J. D. Nelson, "Fabrication of freeform optics," *Optical Manufacturing and Testing XI.* International Society for Optics and Photonics **9575**, 95750H (2015).
4. D. Gurganus, J. D. Owen, B. S. Dutterer, S. Novak, A. Symmons, and M. A. Davies, "Precision glass molding of freeform optics," *Optical Manufacturing and Testing XII.* International Society for Optics and Photonics **10742**, 107420Q (2018).
5. S. C. West, R. Angel, B. Cuerden, W. Davison, J. Hagen, H. M. Martin, D. W. Kim, and B. Sisk, "Development and Results for Stressed-lap Polishing of Large Telescope Mirrors1," *Classical Optics 2014 (2014), Paper OTh2B.4* (Optical Society of America, 2014), p. OTh2B.4.
6. I. Trumper, B. T. Jannuzi, and D. W. Kim, "Emerging technology for astronomical optics metrology," Opt. Lasers Eng. **104**, 22–31 (2018).
7. D. W. Kim, M. Aftab, H. Choi, L. Graves, and I. Trumper, "Optical Metrology Systems Spanning the Full Spatial Frequency Spectrum," (Optical Society of America, 2016), FW5G.4.

Optics EXPRESS

8. M. B. Dubin, P. Su, and J. H. Burge, "Fizeau interferometer with spherical reference and CGH correction for measuring large convex aspheres," (2009), 7426, 74260S–74260S–10.
9. S. Scheiding, M. Beier, U.-D. Zeitner, S. Risse, and A. Gebhardt, "Freeform mirror fabrication and metrology using a high performance test CGH and advanced alignment features," *Advanced Fabrication Technologies for Micro/Nano Optics and Photonics VI*. International Society for Optics and Photonics **8613**, 86130J (2013).
10. R. Huang, P. Su, J. H. Burge, L. Huang, and M. Idir, "High-accuracy aspheric x-ray mirror metrology using Software Configurable Optical Test System/deflectometry," OE, OPEGAR **54**(8), 084103 (2015).
11. D. W. Kim, C. Oh, A. Lowman, G. A. Smith, M. Aftab, and J. H. Burge, "Manufacturing of super-polished large aspheric/freeform optics," (2016), Vol. 9912, pp. 99120F–99120F–9.
12. J. Burke, W. Li, A. Heimsath, C. von Kopylow, and R. B. Bergmann, "Qualifying parabolic mirrors with deflectometry," J. Eur. Opt. Soc. Rapid Publ. **8**, 13014 (2013).
13. C. J. Oh, A. E. Lowman, M. Dubin, G. Smith, E. Frater, C. Zhao, and J. H. Burge, "Modern technologies of fabrication and testing of large convex secondary mirrors," *Advances in Optical and Mechanical Technologies for Telescopes and Instrumentation II*. International Society for Optics and Photonics **9912**, 99120R (2016).
14. S. Chen, S. Xue, Y. Dai, and S. Li, "Subaperture stitching test of convex aspheres by using the reconfigurable optical null," Opt. Laser Technol. **91**, 175–184 (2017).
15. Z. Tian, W. Yang, Y. Sui, Y. Kang, W. Liu, and H. Yang, "A high-accuracy and convenient figure measurement system for large convex lens," Opt. Express **20**(10), 10761–10775 (2012).
16. Y. Chen, E. Miao, Y. Sui, and H. Yang, "Modified Sub-aperture Stitching Algorithm using Image Sharpening and Particle Swarm Optimization," J. Opt. Soc. Korea. **18**, 341–344 (2014).
17. Y.-C. Chen, C.-W. Liang, H.-S. Chang, and P.-C. Lin, "Reconstruction of reference error in high overlapping density subaperture stitching interferometry," Opt. Express **26**(22), 29123–29133 (2018).
18. L. Zhang, D. Liu, T. Shi, Y. Yang, S. Chong, B. Ge, Y. Shen, and J. Bai, "Aspheric subaperture stitching based on system modeling," Opt. Express **23**(15), 19176–19188 (2015).
19. D. Castán-Ricaño, F. S. Granados-Agustín, E. Percino-Zacarías, and A. Cornejo-Rodríguez, "Increase in the measurement of the normal vectors of an aspherical surface used in deflectometry," *Modeling Aspects in Optical Metrology VI*. International Society for Optics and Photonics **10330**, 103301W (2017).
20. I. Scheele, S. Krey, and J. Heinisch, "Measurement of aspheric surfaces with 3D-deflectometry," *Optifab 2007: Technical Digest*. International Society for Optics and Photonics **10316**, 103160P (2007).
21. C. J. Oh, A. E. Lowman, G. A. Smith, P. Su, R. Huang, T. Su, D. Kim, C. Zhao, P. Zhou, and J. H. Burge, "Fabrication and testing of 4.2m off-axis aspheric primary mirror of Daniel K. Inouye Solar Telescope," *Advances in Optical and Mechanical Technologies for Telescopes and Instrumentation II*. International Society for Optics and Photonics **9912**, 99120O (2016).
22. R. Huang, P. Su, T. Horne, G. B. Zappellini, and J. H. Burge, "Measurement of a large deformable aspherical mirror using SCOTS (Software Configurable Optical Test System)," *Optical Manufacturing and Testing X*. International Society for Optics and Photonics **8838**, 883807 (2013).
23. J. Balzer, D. Acevedo-Feliz, S. Soatto, S. Höfer, M. Hadwiger, and J. Beyerer, "Cavlectometry: Towards Holistic Reconstruction of Large Mirror Objects," *2014 2nd International Conference on 3D Vision* 448–455(2014).
24. P. Candry and B. Maximus, "Projection displays: New technologies, challenges, and applications," J. Soc. Inf. Disp. **23**(8), 347–357 (2015).
25. J.-W. Huang, "Design and Fabrication of Ultra-Short Throw Ratio Projector Based on Liquid Crystal on Silicon," Liquid Crystals - Recent Advancements in Fundamental and Device Technologies (2018).
26. B. Martin, J. Burge, S. Miller, S. Warner, and C. Zhao, "Fabrication and Testing of 8.4 m Off-Axis Segments for the Giant Magellan Telescope," (Optical Society of America, 2008), p. OWD6.
27. H. M. Martin, R. G. Allen, J. H. Burge, J. M. Davis, W. B. Davison, M. Johns, D. W. Kim, J. S. Kingsley, K. Law, R. D. Lutz, P. A. Strittmatter, P. Su, M. T. Tuell, S. C. West, and P. Zhou, "Production of primary mirror segments for the Giant Magellan Telescope," *Advances in Optical and Mechanical Technologies for Telescopes and Instrumentation* (International Society for Optics and Photonics, 2014), Vol. 9151, p. 91510J.
28. A. E. Lowman, G. A. Smith, L. Harrison, S. C. West, and C. J. Oh, "Measurement of large on-axis and off-axis mirrors using software configurable optical test system (SCOTS)," *Advances in Optical and Mechanical Technologies for Telescopes and Instrumentation III*. International Society for Optics and Photonics **10706**, 107061E (2018).
29. R. Huang, "High precision optical surface metrology using deflectometry," Ph.D., The University of Arizona (2015).
30. W. H. Southwell, "Wave-front estimation from wave-front slope measurements," J. Opt. Soc. Am. JOSA **70**(8), 998–1006 (1980).
31. W. Zhao, L. R. Graves, R. Huang, W. Song, and D. Kim, "Iterative surface construction for blind deflectometry," *8th International Symposium on Advanced Optical Manufacturing and Testing Technologies: Optical Test, Measurement Technology, and Equipment* (International Society for Optics and Photonics, 2016), **9684**, p. 96843X.
32. L. R. Graves, H. Choi, W. Zhao, C. J. Oh, P. Su, T. Su, and D. W. Kim, "Model-free deflectometry for freeform optics measurement using an iterative reconstruction technique," Opt. Lett., OL **43**, 2110–2113 (2018).

Optics EXPRESS

33. L. R. Graves, H. Choi, W. Zhao, C. J. Oh, P. Su, T. Su, and D. W. Kim, "Model-free optical surface reconstruction from deflectometry data," *Optical Manufacturing and Testing XII*. International Society for Optics and Photonics **10742**, 107420Y (2018).